Steel reinforced composite silicone membranes and its integration to microfluidic oxygenators for high performance gas exchange

Harpreet Matharoo, Mohammadhossein Dabaghi, Niels Rochow, Gerhard Fusch, Neda Saraei, Mohammed Tauhiduzzaman, Stephen Veldhuis, John Brash, Christoph Fusch, and P. Ravi Selvaganapathy

Citation: Biomicrofluidics **12**, 014107 (2018);

View online: https://doi.org/10.1063/1.5014028

View Table of Contents: http://aip.scitation.org/toc/bmf/12/1

Published by the American Institute of Physics

Steel reinforced composite silicone membranes and its integration to microfluidic oxygenators for high performance gas exchange

Harpreet Matharoo,[1,a)] Mohammadhossein Dabaghi,[2,a)] Niels Rochow,[3] Gerhard Fusch,[3] Neda Saraei,[1] Mohammed Tauhiduzzaman,[1] Stephen Veldhuis,[1] John Brash,[2,4] Christoph Fusch,[2,3,5] and P. Ravi Selvaganapathy[1,2]

[1]*Department of Mechanical Engineering, McMaster University, Hamilton, Ontario L8S 4L7, Canada*
[2]*School of Biomedical Engineering, McMaster University, Hamilton, Ontario L8S 4K1, Canada*
[3]*Department of Pediatrics, McMaster University, Hamilton, Ontario L8S 4K1, Canada*
[4]*Department of Chemical Engineering, McMaster University, Hamilton, Ontario L8S 4L7, Canada*
[5]*Department of Pediatrics, Paracelsus Medical University Salzburg, University Hospital Nuremberg, Nuernberg, 90419, Germany*

(Received 14 November 2017; accepted 2 January 2018; published online 11 January 2018)

Respiratory distress syndrome (RDS) is one of the main causes of fatality in newborn infants, particularly in neonates with low birth-weight. Commercial extracorporeal oxygenators have been used for low-birth-weight neonates in neonatal intensive care units. However, these oxygenators require high blood volumes to prime. In the last decade, microfluidics oxygenators using enriched oxygen have been developed for this purpose. Some of these oxygenators use thin polydimethylsiloxane (PDMS) membranes to facilitate gas exchange between the blood flowing in the microchannels and the ambient air outside. However, PDMS is elastic and the thin membranes exhibit significant deformation and delamination under pressure which alters the architecture of the devices causing poor oxygenation or device failure. Therefore, an alternate membrane with high stability, low deformation under pressure, and high gas exchange was desired. In this paper, we present a novel composite membrane consisting of an ultra-thin stainless-steel mesh embedded in PDMS, designed specifically for a microfluidic single oxygenator unit (SOU). In comparison to homogeneous PDMS membranes, this composite membrane demonstrated high stability, low deformation under pressure, and high gas exchange. In addition, a new design for oxygenator with sloping profile and tapered inlet configuration has been introduced to achieve the same gas exchange at lower pressure drops. SOUs were tested by bovine blood to evaluate gas exchange properties. Among all tested SOUs, the flat design SOU with composite membrane has the highest oxygen exchange of 40.32 ml/min m^2. The superior performance of the new device with composite membrane was demonstrated by constructing a lung assist device (LAD) with a low priming volume of 10 ml. The LAD was achieved by the oxygen uptake of 0.48–0.90 ml/min and the CO_2 release of 1.05–2.27 ml/min at blood flow rates ranging between 8 and 48 ml/min. This LAD was shown to increase the oxygen saturation level by 25% at the low pressure drop of 29 mm Hg. Finally, a piglet was used to test the gas exchange capacity of the LAD *in vivo*. The animal experiment results were in accordance with *in-vitro* results, which shows that the LAD is capable of providing sufficient gas exchange at a blood flow rate of ∼24 ml/min. *Published by AIP Publishing.* https://doi.org/10.1063/1.5014028

[a)]H. Matharoo and M. Dabaghi contributed equally to this work.

INTRODUCTION

Respiratory distress syndrome (RDS) is a significant cause of infant mortality even in developed countries. For instance, it has been shown to be the second highest (16%) cause for mortality of infants, who were born with low-weight and suffering from RDS, between the age of one and eighteen years in England and Wales.[1] Respiratory failure under severe RDS is usually treated by mechanical ventilation or extracorporeal membrane oxygenation (ECMO). Intensive mechanical ventilation can cause necrotizing bronchiolitis and alveolar septal injury with inflammation and scarring.[2] As a result, chronic long term complications, i.e., bronchopulmonary dysplasia, can develop which often requires prolonged hospitalization and home oxygen support.[3] ECMO has been shown to significantly reduce mortality in situations where mechanical ventilation is not sufficient. However, the main disadvantage of ECMO is that it requires surgery to connect the device to central blood vessels. Furthermore, ECMO requires systemic anticoagulation, placing the patient at high risk for hemorrhage, in particular, intracranial hemorrhage with related neurological complications.[4] Additionally, the current ECMO devices have a high filling volume requiring priming with donor blood and veno-venous as well as veno-arterial ECMO systems need support by external pumps.[5]

To design such an oxygenator, it should be noted that neonates typically have the arterio venous pressure difference in the range of 20–60 mm Hg (∼30 mm Hg on average), a typical weight of 500 up to 2000 g. A neonate of about 1 kg with RDS will require about 15 to 45 ml/min of their blood to be oxygenated through an external device such as an oxygenator in order to be sustained.[6] Therefore, an ideal oxygenation device for use with preterm infants will have low priming volume, can be pumpless and use the arterio-venous pressure difference to perfuse, have a high surface to volume ratio for high gas exchange, and exchanges gases with the ambient environment, obviating the need for an enriched oxygen atmosphere.[6] A prototype of such a device based on microfluidic oxygenating units was recently described.[2,6] Among reported microfluidic oxygenators,[2,7–18] only those of Wu[18] and Rochow[2] were designed for operation at low pressure and in ambient air. Other devices either required an external blood pump which could lead to additional complications such as hemolysis and erythrocyte damage[19,20] or had an "alveolar" chamber or microchannels [9,10,12–15,17,21] to deliver pure oxygen to the blood to enhance oxygen transfer. Polydimethylsiloxane (PDMS) has been the first choice membrane for all these microfluidic blood oxygenators due to its high permeability to oxygen and carbon dioxide. However, it is elastic and deforms easily which can lead to delamination. This characteristic is particularly detrimental in oxygenators that are exposed to ambient air[18] rather than pressurized enriched oxygen. Increasing the stiffness of the PDMS membrane which is still preserving its oxygen transfer characteristics can be a potential way to improve the performance of such oxygenators. In this paper, we report on a novel composite gas-permeable membrane fabricated by embedding an ultra-thin stainless-steel mesh in PDMS. Additionally, a new design for the blood flow path (referred to as the "vascular network") is introduced to reduce the hydraulic resistance of the single oxygenator unit (SOU) devices while not affecting gas transfer capacity at low blood flow rates. We describe the characteristics and performance of the SOU and lung assist device (LAD) *in vitro* and compare the LAD results of an *in-vivo* animal experiment.

MATERIALS AND METHODS

Design

The oxygenator [also called the lung assist device (LAD)] was designed to be modular to accommodate infants of various weights and consisted of several single oxygenator units (SOUs) combined in series and parallel combinations.

The SOU consisted of a microfluidic vascular network attached to a gas permeable membrane. The vascular network facilitates blood distribution and formation of a thin layer of blood adjacent to the gas permeable membrane to allow oxygenation. Two designs were considered: one in which the height of the channels (100 μm) in the vascular network was uniform [Fig. 1(a)] and the other where the height gradually decreases from the inlet (170 μm) to the center (60 μm)

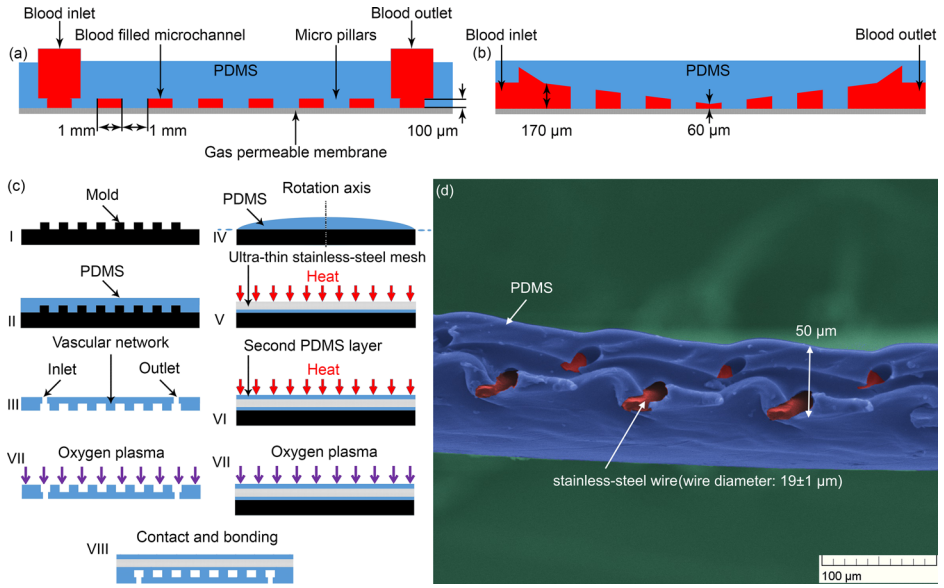

FIG. 1. (a) Schematic cross-sectional view of a flat device, (b) schematic cross-sectional view of a sloping device, (c) device fabrication process, and (d) false colour SEM image of composite membrane.

and then increases to the outlet with 170 μm height [Fig. 1(b)]. The gradual decrease of height from the inlet to the center ensured that there are no deadzones and that there are no sudden changes in the shear stress encountered by the blood. The vascular network was in the shape of a square (43 mm on the side) with the inlet and the outlet connections (4.1 mm inner diameter (ID)) at two diagonally opposite corners and consists of an array of pillars (1 mm $\times$ 1 mm) to support the thin gas permeable membrane attached to it.

PDMS was used as the membrane material due to its high gas permeability.[22] However, thin PDMS membrane bulges out when the microfluidic network is perfused with blood especially when the other side of the membrane is exposed to ambient conditions as in our design. Such deformation can significantly reduce the efficiency of oxygenation and lead to lower saturation levels in the oxygenated blood. Therefore, the PDMS membrane is reinforced with a thin stainless steel mesh (MS-400/19, Asada Mesh Co., Ltd.) that increases its stiffness and prevents deformation under operating pressures. The mesh had a thickness of 39 $\pm$ 2 μm and composite membrane fabricated by infusing the PDMS into the mesh to completely cover it was 50 μm in thickness. The mesh has a pore size of 45 μm and a porosity of 49%.

Fabrication process

Fabrication of the oxygenator is a three-step process as shown in Fig. 1(c): first the vascular network and the membrane are fabricated; the network and the membrane are bonded after the treatment of the surfaces in an oxygen plasma.

The template for the network with flat profile was fabricated by etching the pattern on SU8-100 by means of photolithography[23] [Fig. 1(c.I)]. The vascular network was fabricated by casting PDMS, in 10:1 base/curing agent ratio, on the negative template of the network [Fig. 1(c.II)], at 60 °C for 5 h. After curing, the vascular network was peeled off and residual PDMS inside the tubing was removed [Fig. 1(c.III)]. The template for the network with sloping profile was fabricated on an aluminum block using a ball nose tool of the diameter of 500 μm on a computer numerical control (CNC); 3-axis micro-milling machine (Matsuura LX-1) 1 mm^2 pockets were fabricated using a 500 μm diameter square end micro milling tool on the same machine. The features were machined within 2 μm to 5 μm accuracy.

The PDMS membrane was fabricated by spin-coating PDMS on a substrate made by bonding teflon sheet on silicon wafer. The PDMS was spun at 4000 RPM for 30 s and then cured at

60 °C for 5 h. The composite membrane was fabricated by spinning PDMS at 4000 RPM for 30 s on the substrate [Fig. 1(c.IV)]; the steel mesh was then laid on the uncured material [Fig. 1(c.V)] and cured at 60 °C for 5 h; a second coat of PDMS was then spun onto the mesh [Fig. 1(c.VI)] and cured. The thickness of the resulting membrane was about 50 μm [Fig. 1(d)]. A PDMS membrane without steel mesh reinforcement was also made by bonding two 25-μm-thick layers to produce a combined thickness of 50 μm and used for comparison purposes. In addition, the second 25-μm-thick layer reduced the chance of having any pinholes in PDMS membranes.

The network and the membrane were bonded together by exposing the bonding surfaces to an oxygen plasma at 50 W power for 2.5 min before bringing them into contact [Fig. 1(c.VII)]. The device was dried at 60 °C for 5 h before peeling from the substrate [Fig. 1(c.VIII)].

The LAD consisted of 32 sloping SOUs with composite membranes and included connectors, silicone tubing (MasterFlex platinum-cured silicone tubing), PDMS flow dividers, and acrylic holders. The device included 16 parallel branches containing two SOUs in each branch as shown in Fig. 2(a). The acrylic holders were fabricated using a laser cutter and were glued together using acrylweld (acrylic solvent). Figure 2(b) shows the star-shaped PDMS flow divider designed for optimal blood distribution among the branches as shown in Fig. 2(c). A mold was made using a ProJet^{TM} HD 3000 3D printer (3D SYSTEMS Corp., Rock Hill, USA) and was used to fabricate the flow divider; oxygen plasma was applied to the surfaces for bonding to a thick flat PDMS layer to seal the channels. Blood enters at the center and is distributed among the branches which have a square cross-section with side 1 mm and length 30 mm as depicted in Fig. 2(b). The total priming volume of the LAD was about 10 ml.

Burst pressure and membrane expansion measurement

All the SOUs fabricated were tested at a pressure higher than the operating pressure to ensure that they are structurally sound before integrating them into the LAD or further testing. In order to test the devices, an experimental setup as shown in Fig. 3(a) was constructed. It consisted of a syringe which served as a pressure source attached to the inlet of the SOU. A pressure transducer (TruWave Transducer, Edwards Lifesciences LLC, Irvine, CA, USA) connected to a monitor (SpaceLabs 90369 Patient Monitor, SpaceLabs Medical, Inc.) was also attached to the inlet of the SOU to measure the pressure applied. The SOU was first perfused with water and then the 3-way connector at the outlet was closed to seal the system. The pressure was increased further by pumping more water while monitoring the pressure till reached the maximum of 250 mm Hg. Only the devices that passed this test were used for further testing.

In addition, an optical surface profiler (NewView 5000, Zygo) was used to measure the amount of membrane expansion (deflection) for a sloping SOU with the PDMS membrane at

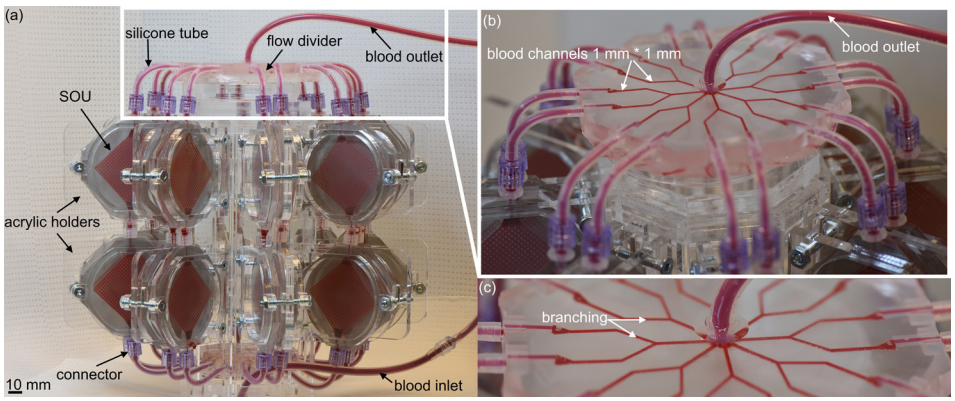

FIG. 2. (a) Image of the LAD with 32 SOUs filled with bovine blood (10 ml total volume), (b) image of the flow divider with 16 branches filled with bovine blood, and (c) close-up view of the flow divider.

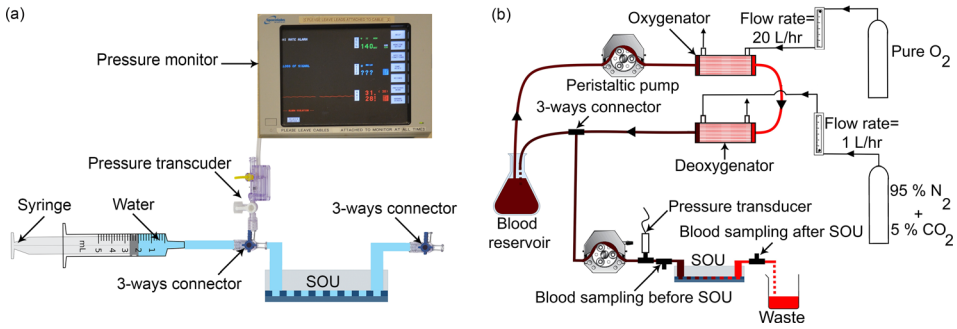

FIG. 3. (a) Experimental setup for burst pressure measurement, (b) experimental setup to test an oxygenator and the LAD.

various applied pressures. After filling SOUs with water and pressuring it to 10, 40, and 70 mm Hg, the topography of the top PDMS membrane was mapped using the optical surface profiler and maximum deflection of the membrane at various locations determined.

In-vitro oxygenation testing

The experimental setup used to characterize oxygenation performance of the SOUs is shown in Fig. 3(b). The setup consists of two parts: the first part consists of a loop used to maintain the oxygen saturation level in blood over the duration of the experiment. The second part of the experimental setup is made of a reservoir, which contains blood, a peristaltic pump, a hollow fiber oxygenator, gas flow regulators, and deoxygenator. Bovine blood (Bovine 7200807-500ML, Lampire Biologics) was used for the experiment and the hematocrit ranged between 28% and 32%. The oxygen saturation, partial pressure of oxygen, partial pressure of carbon dioxide, and pH of the input blood were in the range of 42%–51%, 37–44 mm Hg, 51–61 mm Hg, and 7.07–7.13, respectively. The blood in the reservoir was pumped using a peristaltic pump (ISM832C, Ismatec) through two hollow fiber oxygenators connected in series at a flow rate of 4 ml/min. The first oxygenator (CAPIOX RX05, Terumo) adjacent to the pump was perfused with 20 l/h of oxygen on the gas side to completely oxygenate the blood (to 100% saturation). The deoxygenator (OXR, Living Systems Instrumentation) located downstream was used to set the desired hypoxic condition ($SaO_2 = 46\%$) by flowing a controlled amount of carbon dioxide and nitrogen mixture (5%/95% v/v) through its gas side.

Once the oxygen saturation level of all the blood in the reservoir was stabilized, the blood was withdrawn from the reservoir using a second peristaltic pump (ISM832C, Ismatec) with the setting flow rate ranging between 0.5 and 4 ml/min and pushed through SOUs. When LAD was tested, the blood flow rate was set between 8 and 48 ml/min. Blood was sampled at both the entry and the exit of the tested device and analyzed using a blood gas analyzer (GEM3000, Instrumentation Laboratory). The difference between the oxygen saturation of the blood at the inlet and the outlet was used to calculate the oxygen uptake capacity of the device at the given blood flow rate. For all experiments, the pressure drop was recorded. All experiments were repeated 5 times for each set of conditions.

In vivo experiment

A new born piglet of ~2 kg weight was used to test the LAD using the experimental settings as described previously.[2] Before filling with blood, checks were carried out to ensure that the LAD was leak proof and that all SOUs were perfused equally. The LAD was first filled with isopropanol to remove any air from the device and then the isopropanol was replaced by pumping micro filtered deionized water for 30 min. Subsequently, the LAD was perfused and filled with a normal saline solution containing 3 units/ml heparin. The piglet was anesthetized with intraperitoneal sodium pentobarbital (30 mg/kg; MTC Pharmaceutics, Cambridge, ON, Canada). An ear vein was cannulated with a 22-G angiocatheter (Angiocath, Becton Dickinson, Sandy, UT, USA) for maintenance fluids (5% dextrose at 80 mg/kg day; Baxter, Toronto, ON, Canada) and for

administration of maintenance sodium pentobarbital (16 mg/kg) if needed. An endotracheal tube (size 3.5) was placed via tracheostomy for a mechanical ventilator. Initial settings for the ventilator were set to peak inspiratory pressure (PIP) of 15 mm Hg (2 kPa), positive end-expiratory pressure (PEEP) of 6 mm Hg (0.8 kPa), mean airway pressure (MAP) of 8 mm Hg (1.07 kPa), inspiratory time (IT) of 0.5 s, and respiratory rate (RR) of 30 breaths/min. At baseline, a humidified gas mixture (warmed to 38° C) with FiO_2 of 0.3 was delivered at 8 l/min. Body temperature was maintained constant at 39 °C using a heat lamp and was being monitored by using an ISC probe which was placed on abdomen. A 3.5Fr Argyle umbilical catheter (Sherwood, Medical, St. Louis) was inserted into the right femoral artery to measure systemic blood pressure and heart rate. A bolus of 400 units/kg of heparin was injected to the extracorporeal circuit for anticoagulation; subsequently, heparin was being infused at the flow rate of 30 units/kg h. 14 gauge 1.1 in. length angio-cathethers (BD Catheters) was used to access the left carotid artery and right jugular vein in order to create extracorporeal bypass. Subsequently, the LAD was perfused by being connected to this extracorporeal bypass. The LAD was tested under various flow rates and two different ventilator settings. To simulate respiratory failure and test the efficiency of the LAD, the piglet was ventilated with hypoxic gas ($FiO_2 = 0.15$). Blood samples were collected before and after LAD and analyzed with a blood gas analyzer. The study protocol was approved by the McMaster University Animal Research Ethics Board (AREB#10-03-14).

RESULTS AND DISCUSSION

Oxygenators using the stainless-steel reinforced PDMS membrane were tested for both their mechanical performance and their oxygenation capabilities and compared with oxygenators of similar design but with PDMS membranes without reinforcement. The best performing design of the SOUs was chosen to then build a LAD, consisting of 32 SOUs, and the oxygenation characteristics of the LAD were also tested *in-vitro* at the flow rate similar to those that would be required in a neonate for lung assist function. Finally, the LAD was used in an *in-vivo* experiment to oxygenate a piglet under normoxic and hypoxic conditions.

Mechanical testing

The burst pressure test was conducted on SOUs with flat and sloping channel designs that were attached with both PDMS and composite (PDMS reinforced with stainless steel) membranes. The results, shown in Fig. 4(a), indicate that all the oxygenators are structurally sound and do not fail at pressures that are normally encountered during use (red band in the figure). However, the margin of safety is low for oxygenators that had only the PDMS membrane.

The composite membrane devices demonstrated a significantly better performance and none of the tested devices delaminated or failed in any way even at an applied pressure of 250 mm Hg which is significantly higher than normal operating conditions. The superior performance of composite membrane as compared to PDMS membrane can be attributed to the strength of composite membrane. Figure 4(b) shows schematically a cross-section of the membrane attached to the pillars under pressure "P." The PDMS membrane has a low Young's modulus and undergoes a large deflection under pressure. As a result, the delamination force at the edge of the pillars is directed at a greater angle to the bonded interface which results in peeling of the membrane from the pillars. The composite membrane has higher Young's modulus due to the steel mesh and hence it undergoes a much lower deflection under pressure. As a result, the delamination force is at a lesser angle to the bonded interface. Therefore, it requires a higher force/pressure for delamination making it mechanical more robust.

To quantify the effect of pressure on membrane expansion (deflection), the position of the center point of the membrane in the zone [Fig. 4(c)] between the pillars was measured using the optical profilometer, before and after the application of various pressures ranging from 10 to 70 mm Hg. The change in the position (deflection) of the center point represents the maximum deflection of the membrane in that region to the applied pressure. Zone 1 represents the area at the center of four adjacent pillars located on the corner of a square. The measured deflections are plotted in Fig. 4(d) and show an increase with applied pressure. The deflections

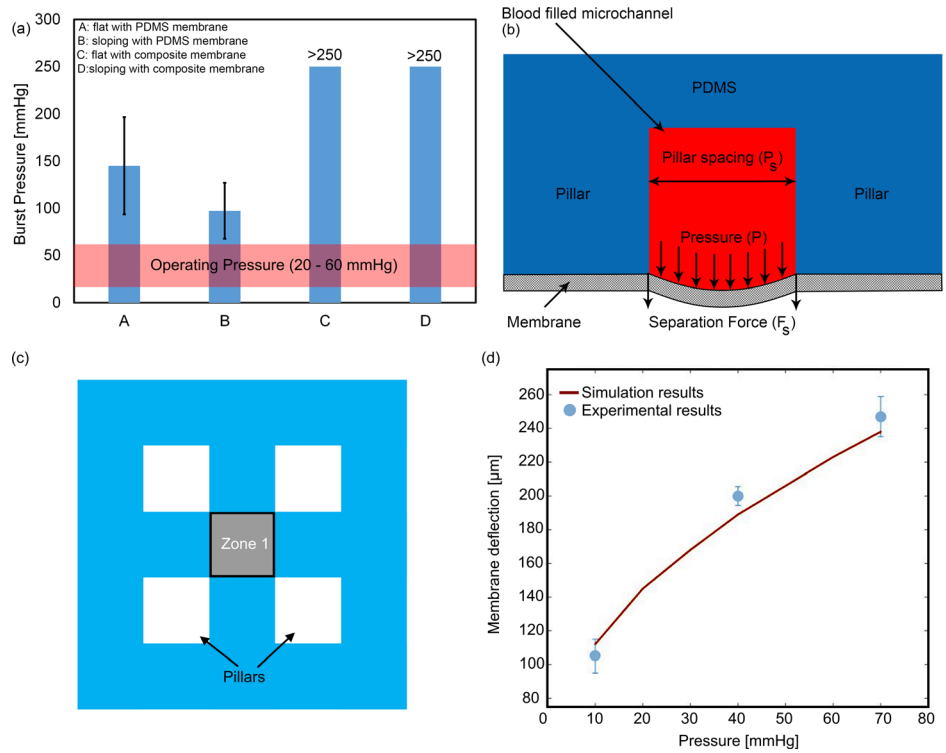

FIG. 4. (a) Burst pressure of oxygenators with various designs. SOUs with composite membrane can sustain higher operating pressure without failure for both flat and sloping designs, (b) figure illustrating a segment of the membrane under pressure, (c) illustration of the zone at which the membrane topography was profiled. The blue regions represent the microchannel network, (d) the amount of membrane expansion (deflection) for three different pressures of 10, 40, and 70 mm Hg for a sloping SOU with PDMS membrane.

are substantial and will have a significant effect on oxygenation. For instance, at a pressure of 40 mm Hg, the effective channel height of a sloping SOU with PDMS will be increased by 200 μm. The measured deflection closely matches with the simulated (using ANSYS) deflection at those applied pressure as shown in Fig. 4(d). Measurements for the composite membrane show negligible deflection of the membrane under these pressure conditions.

In-vitro blood oxygenation measurements for SOUs

Performance of the SOUs was evaluated by flowing blood through them at various set flow rates of 0.5, 1, 1.5, 2, 3, and 4 ml/min while exposing them to the ambient atmosphere. The pressure drop and the increase in the oxygen saturation of the blood between the inlet and the outlet were measured and shown in Fig. 5. The pressure drop [Fig. 5(a)] increases with the flow rate for all the oxygenator designs, as expected. Devices with composite membrane showed higher pressure drop than devices with PDMS membrane. This is again in accordance with expectations since the composite membrane is stiffer and undergoes smaller deflections than the PDMS. Since hydraulic resistance varies inversely with channel height, the hydraulic resistance of devices with composite membrane is expected to be higher than devices with PDMS. The expected pressure drop was also calculated based on a previously published model[24] and was found to be higher than the experimentally obtained value. This is attributed to the expansion of the PDMS which results in a higher effective channel height, reducing the pressure drop observed experimentally. The difference between the calculated pressure drop based on the model and the experimental value is smaller for the composite membrane as compared to the PDMS membrane, indicating that the deflection of the PDMS membrane was larger. The oxygen uptake by the blood [Fig. 5(b)] shows an initial increase to reach a maximum followed by a decrease, for all oxygenator designs. The initial increase can be explained

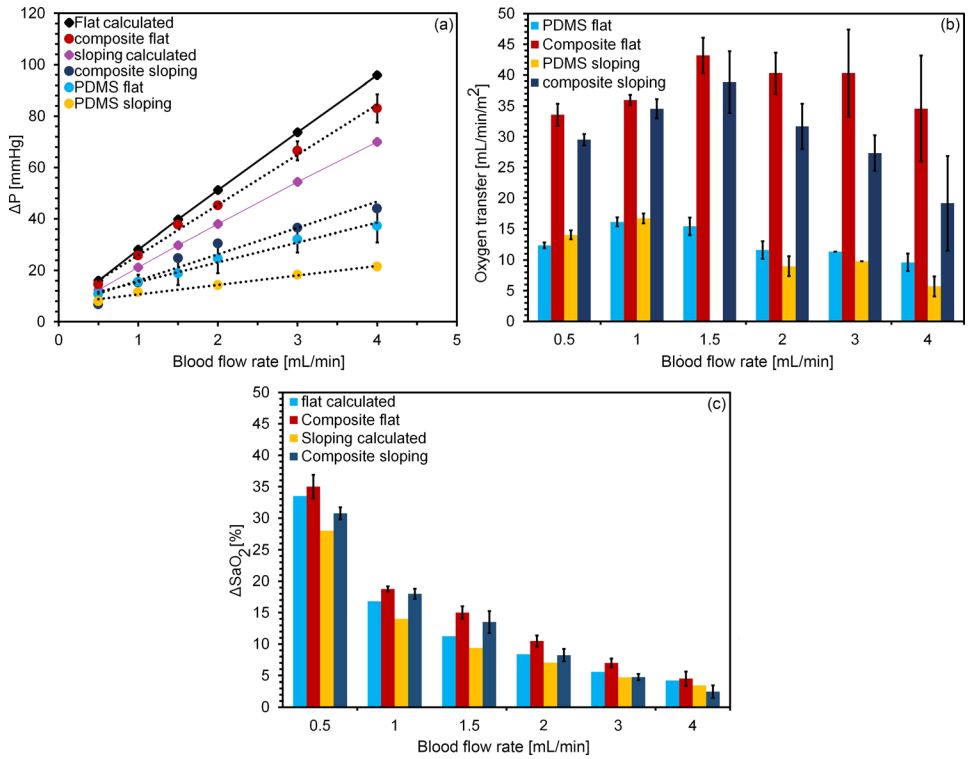

FIG. 5. *In vitro* performance of SOUs: (a) pressure drop, (b) oxygen uptake at various blood flow rates, and (c) comparison of change in the oxygen saturation level (ΔSaO_2) for composite flat and sloping with their calculated values. Data are means ± SD, n = 5.

by the higher flow rate of hypoxic blood that is able to acquire increasing amounts of the oxygen flux through the gas exchange membrane till it reaches the maximum. The decrease in the oxygen uptake at higher flux can be attributed to higher deflection of the membrane at these operating pressures, which reduces the residence time of blood in the device and affects oxygenation performance.

It can also be seen that the SOUs with the composite membrane consisting of steel reinforced PDMS have a higher oxygen uptake than the unreinforced PDMS membrane. The oxygen transfer of both composite flat and sloping SOUs was the same (not statistically different) at low blood flow rates (up to 1.5 ml/min). At higher blood flow rates, composite flat SOUs show better performance compared to composite sloping. However, to make an illustrative comparison between composite flat and sloping designs, an estimation for the performance of each design at an operating pressure of 30 mm Hg, which is the mean expected arterio venous pressure difference in a neonate, should be made. In the case of the flat design with PDMS membrane, the total oxygen uptake was 0.018 ml/min with a flow rate of 3 ml/min. However, the flat design with the composite membrane exhibited the total oxygen uptake of 0.026 ml/min at a flow rate of 1.2 ml/min at an operating pressure of 30 mm Hg which is 44% higher than that of the flat design with PDMS membrane.

The SOU with the sloping design and a composite membrane had a total oxygen uptake of 0.025 ml/min with a flow rate of 1.5 ml/min which was 40% higher than that of the flat design with PDMS membrane. Although the oxygen uptake of the sloping design with composite membrane was nearly the same as the flat profile, it was able to sustain a higher flow rate at the same pressure, thereby enabling oxygenation of more blood. Therefore, this design was selected for fabrication of the LAD.

In addition, the same model[24] was used to calculate the change in oxygen saturation level for both composite flat and sloping designs which were not significantly different from experimental results as shown in Fig. 5(c).

In-vitro blood oxygenation measurements for LAD

To calculate the number of required units for assembling the new LAD, the experimental results for SOUs with sloping design and composite membrane were used. The LAD was supposed to have several parallel branches which would have the same pressure drop as the LAD. In addition, it was assumed that the pressure drop for each branch would split equally between each two SOUs. Then, the number of required branches was calculated to ensure that enough oxygenation at a blood flow rate of 30 ml/min kg of baby would achieve.

The LAD consisting of a total of 32 SOUs with sloping profile and composite membrane assembled in 16 parallel lines with 2 SOUs in series in each line was used to perform pressure drop and blood oxygenation experiments similar to the one's performed for the SOUs. Blood at various flow rates from 8 to 48 ml/min was pumped through the LAD, and the change in oxygen saturation, pressure drop, and CO_2 release (calculated by using change in CO_2 partial pressure) was measured and reported in Fig. 6. It can be seen that in this configuration, the oxygen saturation can be increased by up to 40% at 8 ml/min which reduces with increasing flow rate to ∼13.3% at 48 ml/min [Fig. 6(a)]. This is expected as higher flow rates lead to lower residence time of blood in the oxygenator and hence lesser increase in the saturation level of blood.

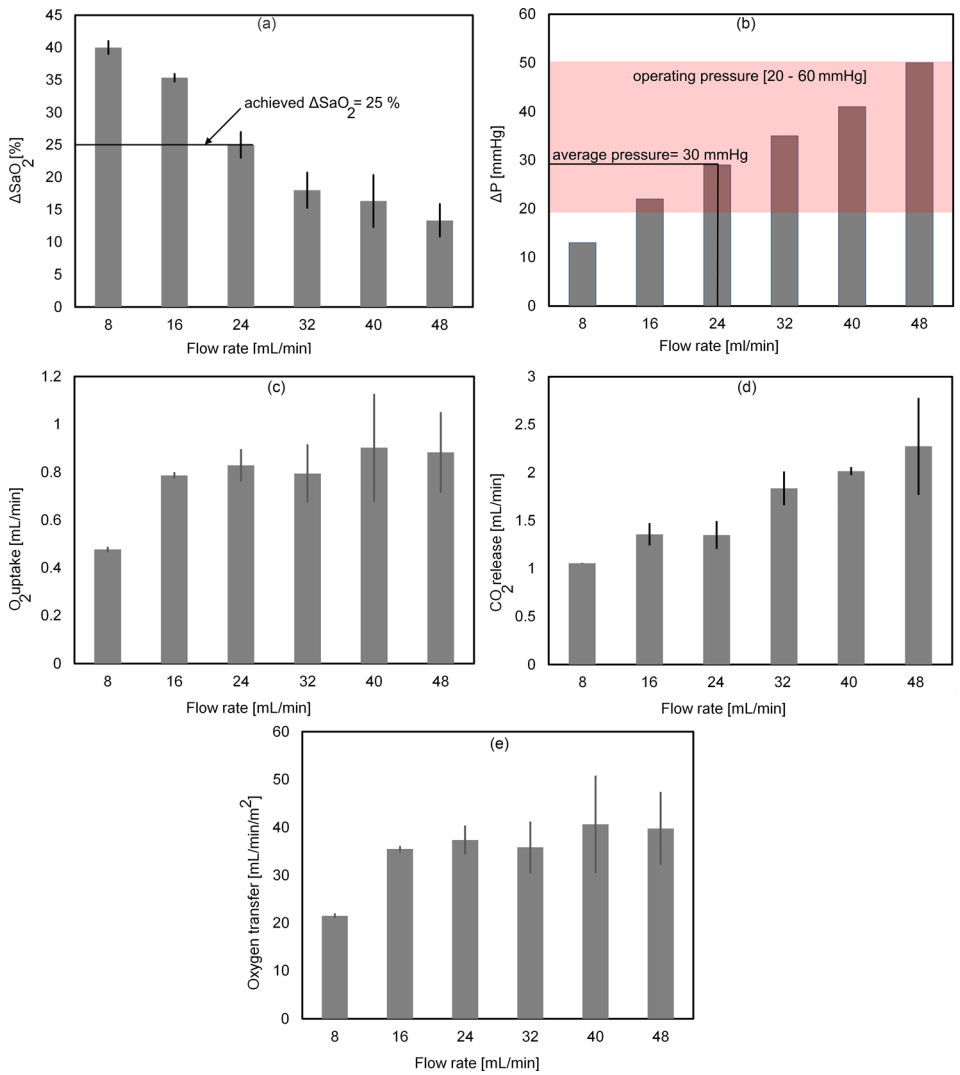

FIG. 6. *In vitro* test of the LAD with bovine blood at various blood flow rates: (a) change in oxygen saturation, (b) pressure drop, (c) oxygen uptake, (d) carbon dioxide release, and (e) oxygen transfer. Data are means ± SD, n = 3.

There is a corresponding increase in the pressure drop from ∼13 mm Hg to 50 mm Hg [Fig. 6(b)]. The oxygen uptake, the CO_2 release, and the oxygen transfer were also found to increase with the flow rate [Figs. 6(c)–6(e)]. This LAD could increase the oxygen saturation level by 25% at a blood flow rate of ∼24 mL/min and an average pressure drop of ∼30 mm Hg, which corresponds to the average oxygen uptake of 0.83 mL/min and CO_2 release of 1.35 mL/min. In comparison, Gimbel and Flores[8] reported an oxygen transfer rate of 1.2 ml/min at a blood flow rate of 25 ml/min for their microfluidic oxygen transfer device using pure oxygen. The microfluidic LAD reported here may be considered more efficient while operating in ambient air given its relatively low pressure drop.

Figure 7 shows oxygen uptake for flat design SOUs with composite membrane tested in ambient air and enriched oxygen atmosphere. Changing air to pure oxygen improved the oxygen uptake of flat design SOUs with composite membrane up to 7 times. Therefore, data for the flat design SOU with composite membrane suggest that in pure oxygen, the oxygen transfer capacity of the LAD would increase by up to 3-fold, meaning that it could achieve oxygen transfer of 2.4 ml/min at a blood flow rate of 24 ml/min.

In order to identify whether the performance of the LAD met the clinical need, the oxygenation requirement was calculated as follows. A typical neonate will have a heart rate of 150 min^{-1} and a stroke volume of 2 ml/kg (body weight).[25] To avoid cardiac compromise, only 10% of cardiac output volume could be sent to the LAD.[26] Therefore, an extracorporeal bypass volume of 30 ml/min kg can be estimated by multiplying heart rate, stroke volume, and percent extracorporeal shunt. This represents the typical flow rate that the LAD has to support and oxygenate.

Assuming an average haemoglobin concentration of 0.16 g/ml (Ref. 18) of blood and oxygen binding capacity of 1.34 ml (oxygen)/g (hemoglobin).[27] Therefore, the total oxygen carrying capacity (0% to 100% saturation) of 30 ml/min kg (Ref. 18) of blood flowing through the LAD would be about 6.4 ml/min kg. Since the typical incoming venous blood into the LAD will be already at 70% saturation in the case of neonates with RDS,[28] increasing the saturation to 100% will require (30% of 6.4) 1.9 ml/min of oxygen uptake. Our current design of LAD achieves an oxygen uptake of 0.83 ml/min in ambient air which could be improved to 2.4 ml/min using pure oxygen. Therefore, if the LAD was operated in an enriched oxygen environment, it is likely to meet the desired oxygen transfer requirement for one kg preterm neonate with RDS.

Comparison to other microfluidic devices

Table I shows the comparison among composite flat, composite sloping, and the LAD presented in this study with other microfluidic blood oxygenator devices which used air as ventilating gas.[2,16,17,29] In this comparison, oxygen transfer and blood flow rate are normalized to the

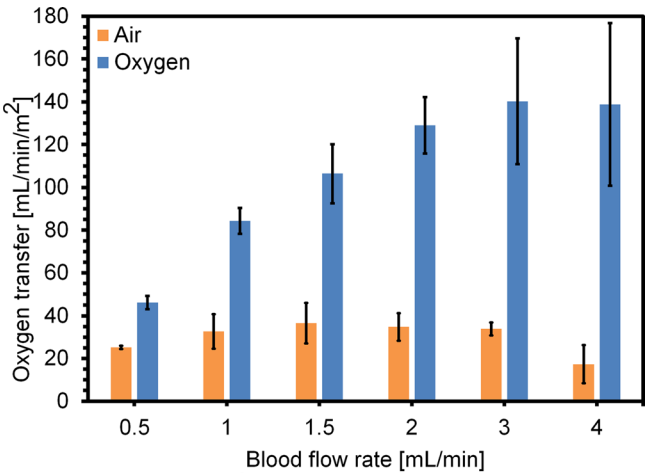

FIG. 7. *In vitro* performance of flat design SOUs with composite membrane and the channel height of 110 μm tested in air and pure oxygen.

TABLE I. A summary of previous works of microfluidic blood oxygenator devices. This table includes only devices which were tested by air. Values in the table are from each reported work or estimated based on reported values in each work. The height of blood channels is shown by H. The oxygen transfer and pressure drop data represent the maximum reported results at achieved blood flow rates for that oxygen transfer. N/A indicates that these data were not available from the papers.

	H (μm)	Surface area (cm^2)	Priming volume (ml)	ΔP (mm Hg)	Oxygen transfer (ml/min m^2)	Flow rate (l/min m^2)
Composite flat	100	7.04	0.14	83	40.32	5.68
Composite sloping	170–60	6.93	0.166	44	38.88	5.77
LAD	170–60	221.76	10	50	40.67	2.16
Potkay[16]	20	2.34	0.006	500	138.9	6.41
	10	1.67	0.002	N/A	224.5	8.98
Rochow[2]	80	152.6	4.8	62	31	2.62
Rieper[17]	200	1200	7	80	13	0.5
Thompson[29]	10	N/A	N/A	120	44	2.64

effective gas exchange surface area to provide a better comparison among all devices. As shown in Table I, the LAD has better oxygen transfer at the same normalized blood flow rate compared to others except Potkay[16] 2011 and Rieper[17] 2015. However, it should be noted that the higher oxygen transfer in these studies was achieved at a high pressure drop of 500 mm Hg and 80 mm Hg, respectively, which are not suitable for using as a pumpless device in neonatal intensive care unit (NICU) for preterm and term neonates suffering from RDS.

In-vivo animal experiments

The LAD was then connected to a piglet and its oxygenation performance tested under various flow rates and two different ventilator settings: (i) the piglet was ventilated under standard condition (oxygen was fed into the mechanical ventilator) and (ii) hypoxic gas was used to simulate lung failure ($FiO_2 = 0.15$) using experimental set-up shown in Fig. 8. The oxygen partial pressure (PO_2), carbon dioxide partial pressure (PCO_2), and oxygen saturation level (SaO_2) were measured during the experiment both before and after the blood enters the LAD as reported in Table II.

At baseline setting a maximum blood flow rate of 25 ml/min was achieved. The mean arterial blood pressure was 48 mm Hg, and the mean pressure in the tube between carotid artery and the LAD was 32 mm Hg. The LAD raised oxygen saturation from SaO_2 91%–98% to 100%. The LAD was tested for 150 min under this condition. Further, the LAD was tested under hypoxic ventilation of the piglet ($FiO_2 = 0.15$). A maximum flow rate of 16.7 ml/min with a mean arterial blood pressure of 29 mm Hg was achieved. It is notable that the LAD was able to raise the oxygen saturation (SaO_2) level from 56% to 69% to 98%–100%. In addition, at lower flow rates of 11 and 15 ml/min, the oxygen saturation could be increased to near complete saturation from a

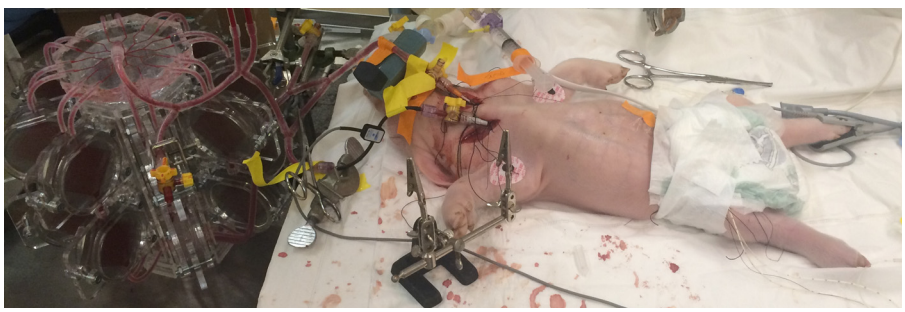

FIG. 8. Setup of the animal experiment.

TABLE II. Blood gases measured during the animal experiment at the inlet (blood from piglet to LAD) and the outlet of the LAD.

Sample	Blood flow rate (ml/min)	Pre-LAD PCO_2 (mm Hg)	Pre-LAD PO_2 (mm Hg)	Pre-LAD SaO_2 (%)	Post-LAD PCO_2 (mm Hg)	Post-LAD PO_2 (mm Hg)	Post-LAD SaO_2 (%)
Normal condition							
1	10	42	72	93	17	169	100
2	13.7	35	60	91	13	199	100
3	16	41	65	93	20	180	100
4	16.7	45	88	98	19	181	100
5	18.3	40	75	95	24	178	100
6	24	43	72	94	26	175	100
7	25	41	77	95	24	198	100
Hypoxic gas ($FiO_2 = 0.15$)							
1	11	45	33	56	27	160	98
2	15	41	33	60	25	125	99
3	16.7	39	38	69	23	105	100

lower value of 56% and 60%. The duration of the hypoxia experiment was 50 min. The total *in-vivo* experiment during which the piglet was stable lasted in total 5 h.

The *in-vivo* performance of the LAD under the hypoxic conditions (SaO_2: 69% to 100% at 16.7 ml/min) is comparable to the *in-vitro* experiment results of the LAD (SaO_2: 58% to 93%–94% at 16 ml/min).

CONCLUSION

In this study, a steel mesh-reinforced composite silicone membrane was introduced to improve the performance of a microfluidic blood oxygenator in terms of mechanical strength of the membrane and oxygenation. A new design with a "sloping" flow profile of the blood flow channels was developed to reduce flow resistance. In addition, a new LAD design having 32 individual oxygenator units with composite membranes and sloping profiles connected in parallel was built and tested. Composite membrane devices showed improvement in oxygenation of up to 44% compared to PDMS membrane devices. At a mean pressure of 30 mm Hg, the LAD increased oxygenation by 25% at a blood flow rate of 24 ml/min. In addition, *in vivo* experiment results were in accordance with *in vitro* blood experiment results, and both of them showed that the performance of the LAD was significantly improved. The design is amenable to further reduction in the form factor in order to make it more compact. These simple and passive oxygenation devices which do not require an external pump or enriched oxygen supply are likely to find broad applications for oxygenation not only with neonates but also with infants and in some cases adults.

ACKNOWLEDGMENTS

The authors acknowledge the support of the Natural Sciences and Engineering Research Council of Canada (NSERC) and Canadian Institutes for Health Research (CIHR) through their CHRP program for funding this project. P.R.S. also acknowledges the Canada Research Chairs Program for support.

[1]W. J. Watkins, S. J. Kotecha, S. Kotecha, M. Winkleby, and S. Petrou, PLoS Med. **13**, e1002018 (2016).
[2]N. Rochow, A. Manan, W.-I. Wu, G. Fusch, S. Monkman, J. Leung, E. Chan, D. Nagpal, D. Predescu, J. Brash, P. R. Selvaganapathy, and C. Fusch, Artif. Organs **38**, 856 (2014).
[3]R. J. Rodriguez, Respir. Care **48**, 279 (2003).
[4]A. Polito, C. S. Barrett, D. Wypij, P. T. Rycus, R. Netto, P. E. Cogo, and R. R. Thiagarajan, Intensive Care Med. **39**, 1594 (2013).

[5]R. de Vroege, M. Wagemakers, H. te Velthuis, E. Bulder, R. Paulus, R. Huybregts, W. Wildevuur, L. Eijsman, W. van Oeveren, and C. Wildevuur, ASAIO J. **47**, 37 (2001).
[6]N. Rochow, E. C. Chan, W.-I. Wu, P. R. Selvaganapathy, G. Fusch, L. Berry, J. Brash, A. K. Chan, and C. Fusch, Int. J. Artif. Organs **36**, 377 (2013).
[7]T. Femmer, M. L. Eggersdorfer, A. J. Kuehne, and M. Wessling, Lab Chip **15**, 3132 (2015).
[8]A. A. Gimbel, E. Flores, A. Koo, G. García-Cardeña, and J. T. Borenstein, Lab Chip **16**, 3227 (2016).
[9]D. M. Hoganson, J. L. Anderson, E. F. Weinberg, E. J. Swart, B. K. Orrick, J. T. Borenstein, and J. P. Vacanti, J. Thorac. Cardiovasc. Surg. **140**, 990 (2010).
[10]D. M. Hoganson, H. I. Pryor, E. K. Bassett, I. D. Spool, and J. P. Vacanti, Lab Chip **11**, 700 (2011).
[11]L. F. M. J.-K. Lee, M. C. Kung, and H. H. Kung, ASAIO J. **54**, 390 (2008).
[12]T. Kniazeva, A. A. Epshteyn, J. C. Hsiao, E. S. Kim, V. B. Kolachalama, J. L. Charest, and J. T. Borenstein, Lab Chip **12**, 1686 (2012).
[13]T. Kniazeva, J. C. Hsiao, J. L. Charest, and J. T. Borenstein, Biomed. Microdevices **13**, 315 (2011).
[14]K. M. Kovach, M. A. LaBarbera, M. C. Moyer, B. L. Cmolik, E. van Lunteren, A. Sen Gupta, J. R. Capadona, and J. A. Potkay, Lab Chip **15**, 1366 (2015).
[15]J. K. Lee, H. H. Kung, and L. F. Mockros, ASAIO J. **54**, 372 (2008).
[16]J. A. Potkay, M. Magnetta, A. Vinson, and B. Cmolik, Lab Chip **11**, 2901 (2011).
[17]T. Rieper, C. Muller, and H. Reinecke, Biomed. Microdevices **17**, 1 (2015).
[18]W.-I. Wu, N. Rochow, E. Chan, G. Fusch, A. Manan, D. Nagpal, P. R. Selvaganapathy, and C. Fusch, Lab Chip **13**, 2641–2650 (2013).
[19]J. Byrnes, W. McKamie, C. Swearingen, P. Prodhan, A. Bhutta, R. Jaquiss, M. Imamura, and R. Fiser, ASAIO J. **57**, 456 (2011).
[20]A. D. Meyer, A. A. Wiles, O. Rivera, E. C. Wong, R. J. Freishtat, K. Rais-Bahrami, and H. J. Dalton, Pediatr. Crit. Care Med. **13**, e255 (2012).
[21]M. C. Kung, J.-K. Lee, H. H. Kung, and L. F. Mockros, ASAIO J. **54**, 383 (2008).
[22]M. C. Bélanger and Y. Marois, J. Biomed. Mater. Res. **58**, 467 (2001).
[23]H. Lorenz, M. Despont, N. Fahrni, N. LaBianca, P. Renaud, and P. Vettiger, J. Micromech. Microeng. **7**, 121 (1997).
[24]J. A. Potkay, Biomed. Microdevices **15**, 397 (2013).
[25]Y. Agata, S. Hiraishi, K. Oguchi, H. Misawa, Y. Horiguchi, N. Fujino, K. Yashiro, and N. Shimada, J. Pediatr. **119**, 441 (1991).
[26]Y. Takahashi, K. Harada, A. Ishida, M. Tamura, T. Tanaka, and G. Takada, Early Hum. Dev. **44**, 77 (1996).
[27]R. N. Pittman, "Oxygen transport," in *Regulation of Tissue Oxygenation.* San Rafael (CA) (Morgan & Claypool Life Sciences, San Rafael (CA), 2011), Chap. 4.
[28]M. Zimmermann, T. Bein, A. Philipp, K. Ittner, M. Foltan, J. Drescher, F. Weber, and F. X. Schmid, Br. J. Anaesth. **96**, 63 (2006).
[29]A. J. Thompson, L. H. Marks, M. J. Goudie, A. Rojas-Pena, H. Handa, and J. A. Potkay, Biomicrofluidics **11**, 024113 (2017).